QUARTERLY JOURNAL OF THE ROYAL METEOROLOGICAL SOCIETY
Q. J. R. Meteorol. Soc. **133**: (S1) 85–95 (2007)
Published online in Wiley InterScience
(www.interscience.wiley.com) DOI: 10.1002/qj.126

RMetS
ROYAL METEOROLOGICAL SOCIETY

Comparison of AATSR and SEVIRI aerosol retrievals over the Northern Adriatic

G. E. Thomas,[a]* C. A. Poulsen,[b] R. L. Curier,[c] G. de Leeuw,[c] S. H. Marsh,[a] E. Carboni,[a] R. G. Grainger[a] and R. Siddans[b]

[a] *University of Oxford, UK*
[b] *Rutherford Appleton Laboratory, UK*
[c] *TNO Defence, Security and Safety, The Netherlands*

ABSTRACT: A case-study is presented comparing the Oxford–RAL retrieval of Aerosol and Cloud (ORAC) algorithm, applied to AATSR and Meteosat-8 SEVIRI data, and the dual-view AATSR aerosol retrieval developed at TNO. The study compares data from an AATSR overpass of the Northern Adriatic and Po Valley region on 4 September 2004, during which time there were two AERONET sunphotometer stations operating in the Venice region as part of the ADRIEX campaign.

We present the results of a comparison of the optical depth determined from the two AATSR retrievals and the SEVIRI retrieval at the time of the AATSR overpass. The comparison shows that the satellite retrievals consistently overestimate the aerosol optical depth compared to the AERONET site. A possible reason for this over sea is an inability of the algorithms at present to take into account the ocean colour of coastal waters. Future improvements to the algorithms are suggested. Copyright © 2007 Royal Meteorological Society

KEY WORDS ADRIEX; AERONET; aerosol optical depth

Received 16 May 2006; Revised 4 June 2007; Accepted 7 June 2007

1. Introduction

Atmospheric aerosols play an important role in determining both local air quality and the radiative balance of the Earth's atmosphere, but their distribution, composition and evolution are still relatively poorly understood. The radiative impact of aerosols, both through direct forcing and interaction with cloud processes, is believed to be a negative forcing (i.e. cooling) of a similar magnitude to the forcing due to anthropogenic enhancement of greenhouse gas concentrations. However, the uncertainty in the aerosol forcing is very large and the level of understanding very poor (IPCC, 2001; Lohmann and Feichter, 2005). The use of satellite measurements to provide global observations of aerosols is a key element in improving our understanding of the effects of aerosols on the Earth's radiation budget. Additionally, satellite measurements offer the ability to detect and track aerosol events – which can result in significant air quality problems – on a regional scale.

Early attempts to measure column aerosol properties from visible/infrared satellite instruments were limited to estimating aerosol optical depth (AOD) over the ocean, by comparing the radiance measured in one or two narrow wavebands to modelled clear-sky radiances. The most notable datasets of this nature are those derived from the Advanced Very High Resolution Radiometer (AVHRR) series of instruments flown on the NOAA satellites since 1981. Initially, AOD was derived from a single channel, based on the principle that, over dark surfaces, the variation in upwelling radiance in the visible is dominated by the AOD (Stowe *et al.*, 1997). The algorithm has since been extended to include a second channel and to retrieve the Ångström parameter as well as optical depth (Mishchenko *et al.*, 1999).

More recently, instruments such as the Moderate Resolution Imaging Spectroradiometer (MODIS, on board NASA's Terra and Aqua platforms), Multi-angle Imaging Spectroradiometer (MISR, on board Terra alone) and (Advanced) Along Track Scanning Radiometer (ATSR-2 on ERS-2; AATSR on Envisat) have utilized multiple-channel and multiple-viewing-angle algorithms to extend the coverage of operational aerosol products to the land as well. MODIS (Remer *et al.*, 2005) utilizes its relatively high spectral resolution (the instrument has 36 bands in the visible and infrared) to decouple the surface and atmospheric contribution to the signal, based on empirical relationships between pairs of channels. Over land, an aerosol model is then selected from an ensemble, again using empirically derived relationships between channels, and a look-up table is used to compute the optical depth for that aerosol class. Over the ocean a different approach is taken; here a two-component aerosol is generated by fitting a radiance look-up table made up of four 'fine' aerosol modes and five 'coarse' ones. The fine–coarse

* Correspondence to: G. E. Thomas, Atmospheric, Oceanic and Planetary Physics, Clarendon Laboratory, Parks Road, Oxford OX1 3PU, UK. E-mail: gthomas@atm.ox.ac.uk

mode combination selected is that which provides the best match to the measurements, as a function of optical depth, reflectance weighting parameter and aerosol effective radius. A somewhat similar aerosol algorithm has also been developed for the Medium Resolution Imaging Spectrometer (MERIS – a similar instrument to MODIS – which is on board Envisat; Höller *et al.*, 2005), however these data are not yet widely available.

The MISR instrument (Martonchik *et al.*, 2002) approaches the problem of variable surface reflectance by utilizing nine views of the same scene at different viewing angles and four visible/near-infrared wavebands. These measurements are then used to fit both the atmospheric path radiance (related to a series of prescribed aerosol classes) and the surface reflectance. By selecting the aerosol class which best matches the measured radiances, an optical depth and aerosol class are determined.

However, all of these products have limitations – for instance the MODIS algorithm performs poorly over bright surfaces, while MISR has relatively poor spatial coverage due to its narrow swath. These limitations, added to the need for improved global coverage (due to the high degree of both spatial and temporal variability in aerosol), means that there is a clear need for the development of further satellite aerosol products.

The derivation of aerosol properties from imaging satellite sensors requires assumptions to be made about the aerosol composition, size distribution and height distribution, as well as the radiative properties of the underlying surface. Such assumptions inevitably introduce errors into the derived aerosol products, and these are difficult to characterize without extensive validation against both ground-based and independent satellite measurements. Ground-based measurements (most notably the Aerosol Robotic Network (AERONET) of sunphotometers; Holben *et al.*, 1998) typically provide high-accuracy measurements of AOD at several wavelengths, as well as other derived products, but make measurements at only one location. Comparing retrievals of aerosol properties from a single scene using multiple satellite sensors and analysis algorithms, in conjunction with ground-based measurements within the scene, should provide more insight into the different satellite products than a simple comparison with ground-based measurements alone.

We present one such intercomparison for measurements made by the AATSR and the Spinning Enhanced Visible Infrared Radiometer (SEVIRI) during the Aerosol Direct Radiative Impact Experiment (ADRIEX) campaign described in detail in Highwood *et al.* (2007). On 4 September 2004, AATSR captured data over the ADRIEX study area while both AERONET sunphotometers within the area were under clear skies. From the two instruments, three separate aerosol products have been generated: the Oxford/RAL Aerosol and Clouds (ORAC) optimal estimation algorithm has been applied to both AATSR and SEVIRI data, and the dual-view algorithm developed by TNO has been applied to AATSR data.

Both algorithms used in this comparison have their own advantages and weaknesses. As the ORAC algorithm uses an optimal estimation framework (Rodgers, 2000), it will provide the 'best' possible match to the measured radiances, given all the available information (i.e. it will provide the *a posteriori* solution to the problem of fitting the forward model to the radiances, taking the *a priori* information into account). However, as it is a single-view algorithm, it relies on good knowledge and accurate modelling of the surface reflectance. The TNO algorithm is a more *ad hoc* method and, if the reflectance characteristics of the surface were well known, ORAC would be expected to outperform it. However, by using the dual-view capability of the AATSR measurements to effectively decouple the surface and atmospheric contributions, the method is much less dependent on accurate surface reflectance modelling. By comparing these two algorithms applied to the same data, and with independent ground-truth measurements provided by the two AERONET sunphotometers, the following questions can be addressed:

- How big a limiting factor is the description of the land's surface reflectance in the ORAC retrieval?
- Is the assumption used to decouple the land and atmospheric signal in the dual-view retrieval reliable, or is there evidence of areas where the assumption is not applicable?
- Can the differing approaches of each algorithm reveal any ways in which they can both be improved?

The addition of ORAC retrievals from the geostationary SEVIRI instrument is another aspect to this study. Geostationary satellites capable of producing measurements suitable for this type of analysis are a relatively new development, and one with great potential. Geostationary platforms offer the ability to monitor a large portion of the globe on an almost continuous basis. Comparing results from a geostationary platform with those from a polar-orbiting instrument using the same retrieval algorithm could reveal unforeseen effects of the differing viewing geometry and larger pixel size of the geostationary instrument.

2. Instrument and algorithm descriptions

2.1. AATSR

AATSR is the third instrument in a series of visible/infrared imaging radiometers and is primarily designed to measure sea surface temperature to the accuracy required for long-term climate monitoring. AATSR is on board the European Space Agency (ESA) polar-orbiting Envisat platform, which was launched in March 2002. (The preceding instruments, ATSR-1 and ATSR-2, flew on board the ESA ERS-1 and ERS-2 satellites, respectively.) One of the unique features of the (A)ATSR instruments is their dual-view scanning pattern, whereby the same region of the surface is imaged firstly at a zenith

DOI: 10.1002/qj

angle of approximately 55° and then again, approximately 90 s later, in a nadir view.

AATSR has 7 channels at 0.55, 0.67, 0.87, 1.6, 3.7, 11.0, 12.0 μm and provides a 512 km swath with a nadir-view resolution of 1×1 km^2. Only channels 1–4 (i.e. the visible/near-infrared channels) are used for aerosol retrievals in the analysis presented here (the thermal infrared channels are used in cloud flagging). Envisat is in a sun-synchronous orbit with an overpass time of 11:00 local solar time.

The (A)ATSR instrument series provide 11 years (and counting) of continuous global data suitable for aerosol retrieval, which means these data predate the MODIS and MISR datasets by 5 years. Additionally, the dual-viewing geometry of this instrument makes it ideally suited to making aerosol measurements over land. The primary disadvantage of these instruments is their relatively narrow swath width (a consequence of the dual-view system), which means they can provide gobal coverage once every three days at best.

As well as the two algorithms discussed here, a third algorithm for deriving aerosol properties from (A)ATSR measurements has been developed by North (2002). This uses a different approach to both methods used here by retrieving the AOD and surface reflectance using the dual view and a parametrization of the variation of the land's surface reflectance with viewing angle.

2.2. SEVIRI

SEVIRI (Aminou *et al.*, 1997) is a line-scanning radiometer located on board the European geostationary meteorological satellites Meteosat-8 and -9. Meteosat-8 was launched in 2003 and the first data were available in early 2004 and it is from this satellite that the data used here originated. (Meteosat-9 was launched in December 2005 and replaced Meteosat-8 as the primary Meteosat in mid-April 2007.) The instrument provides data in four visible and near-infrared channels and 8 infrared channels with a resolution of 3 km at the sub-satellite point. The channels used in the analysis presented here are 0.635, 0.81 and 1.6 μm. A key feature of SEVIRI is its ability to continuously image the Earth every 15 minutes. This allows aerosol events, such as dust storms, to be tracked in near-real time, which offers a great advantage over polar-orbiting instruments. The main disadvantage of this instrument is the susceptibility of the larger field of view to contamination by cloud and lack of dual-view capability.

The potential of SEVIRI as an instrument for aerosol remote sensing has been demonstrated by two independant applications of AVHRR-style aerosol retrievals over the ocean (Thieuleux *et al.*, 2005; Brindley and Ignatov, 2006). The studies showed promising agreement between ground-based and other satellite measurements, but the method is limited to ocean retrievals.

2.3. TNO dual-view algorithm

The TNO algorithm for aerosol retrieval over land in cloud-free conditions (see Robles Gonzalez, 2003, for cloud screening over land) has been developed to retrieve aerosol properties such as the AOD and the mixing ratio of the dominant aerosol classes from ATSR-2 and AATSR data. This procedure is based on aerosol models describing the aerosol microphysical and optical properties, determined by the chemical composition, to calculate the reflectance at the top of the atmosphere (TOA) using a radiative transfer model. The radiative transfer model used at TNO is the DAK model (De Haan *et al.*, 1987; Stammes, 2001) developed at KNMI. For this study a bimodal aerosol distribution was used defined by two log-normal distributions centred at 30 and 50 nm, with optical properties based on those given by Volz (1972). The TOA reflectance is calculated for each of the aerosol classes that are expected to occur in the area of interest, based on *a priori* knowledge or on climatology. A further assumption is that the aerosol particles are spherical so Mie theory (Mie, 1908) applies for the calculation of the aerosol extinction. The TOA reflectances determined from the radiance measured with ATSR are compared with the weighted average of the modelled reflectances for two different aerosols models at the wavelengths 0.55, 0.67 and 1.6 μm. The error function for all three wavelengths is minimized for a range of aerosol class mixing ratios to determine both the spectral AOD and the aerosol mixing ratio. The AOD wavelength dependence is expressed by the Ångström parameter. The aerosol retrieval algorithm is based on two assumptions:

- The reflectance TOA due to an external mixture of two aerosol classes is the weighted average of the reflectance TOA of each of the aerosol classes (Wang and Gordon, 1994).
- The reflectance TOA can be approximated as a linear function of the AOD with the reflectance of an aerosol-free atmosphere as an offset (Durkee *et al.*, 1986).

With these assumptions and knowledge on the aerosol optical properties, the AOD can be directly determined over a dark surface, such as deep ocean or dark vegetation, using a single view (Veefkind and De Leeuw, 1998). Over brighter surfaces, the effects of the surface reflection and the atmospheric reflection on the TOA reflectance need to be separated. This is accomplished by taking advantage of the two views provided by ATSR. In the so-called dual-view algorithm it is assumed that k, the ratio between the reflectance in the nadir view and the reflectance in the forward view, is independent of the wavelength (Flowerdew and Haigh, 1995). A limitation of this approximation is that it fails at wavelengths where there is strong reflectance from vegetation. For this reason the TNO algorithm does not make use of the 0.87 μm channel.

The dual-view algorithm has been tested for the retrieval of the AOD and the Ångström parameter over

DOI: 10.1002/qj

several regions by comparison with AERONET data (Veefkind *et al.*, 1998; Robles Gonzalez *et al.*, 2000; Robles Gonzalez *et al.*, 2006). It was developed for the ATSR-2 and has been updated for using AATSR data. The single- and dual-view algorithms are combined in a single quasi-operational algorithm for application to large datasets. The application of the algorithm to the retrieval of the mixing ratio of the dominant aerosol classes is more difficult to test, since this requires information on the occurrence of aerosol composition over the area. A first attempt was made over the Indian Ocean, using data from the Indian Ocean Experiment (INDOEX). The results show the variation of the mixing ratio with wind fetch over the ocean, from a single industrial aerosol class near the Indian continent to an aerosol class dominated by sea-spray aerosol near the Intertropical Convergence Zone (Robles-Gonzalez *et al.*, 2006). In this paper we present only the spectral AOD and its validation using AERONET data.

2.4. AATSR ORAC algorithm

The ORAC algorithm (Thomas *et al.*, 2007) is an optimal estimation scheme designed to allow the retrieval of aerosol and/or cloud properties from near-nadir satellite radiometers, developed from the Enhanced Cloud Processor (Watts *et al.*, 1998). The retrieval uses the Levenburg–Marquardt algorithm to fit modelled radiances to the satellite measurements in a combination of visible/near-infrared channels. The forward model is based on the plane-parallel radiative transfer code DISORT (Stamnes *et al.*, 1988) and accounts for both gas absorption (as given by MODTRAN for a single reference atmosphere (Berk *et al.*, 1998) and Rayleigh scattering. Aerosol scattering is modelled using Mie scattering theory and a 30-layer aerosol profile. Aerosol microphysical properties are based on the Global Aerosol Data Set (GADS) included with the Optical Properties of Aerosol and Cloud package (Hess *et al.*, 1998). The scheme uses surface reflectances based on the MODIS bidirectional reflectance distribution function (BRDF) product (Jin *et al.*, 2003) over land and an ocean reflectance model based on Cox and Munk (1954) wave statistics. Validation of the ORAC aerosol retrieval is an ongoing process, with early results being presented in Kokhanovsky *et al.* (2007).

The primary parameters retrieved by ORAC are AOD at 0.55 μm and effective radius. In addition, the algorithm allows small changes in the overall surface reflectance, although the spectral shape of the surface is fixed. In the configuration used in this analysis, the retrieval also returns the optical depth at 0.87 μm. This is calculated using a look-up table of the extinction coefficient at 0.55 μm and 0.87 μm for the appropriate aerosol class, as a function of 0.55 μm optical depth and effective radius. Cloud flagging has been performed using the ESA operational cloud flag (Birks *et al.*, 2004) over the ocean, while land pixels have been cleared using quality controls on the retrieved product. The ability to perform post-retrieval cloud flagging is a feature which results from the optimal estimation method employed in ORAC. As the forward model is unable to accurately simulate the radiances measured from cloud-filled pixels, the retrieval will either fail to converge, or will converge with an abnormally high cost. Filtering the retrieved product by cost has been found to be a very effective cloud flag and is particularly useful over land pixels, although it does add a significant computational overhead. A number of different aerosol classes (continental, desert, maritime and biomass burning) were used to estimate the AOD and the case with the best fit as defined by the algorithm was used in the comparison with AERONET data.

2.5. SEVIRI ORAC algorithm

The ORAC algorithm has also been applied to SEVIRI data; however, as SEVIRI lacks a 0.55 μm channel, only the 0.67, 0.87 and 1.6 μm channels are currently used to derive aerosol optical properties. A sub-selection of the channels is used to determine the cloud mask, using the operational EUMETSAT cloud flagging scheme, supplemented by additional quality control from the optimal estimation algorithm. The same aerosol classes used in the ORAC/AATSR retrievals were also used in the SEVIRI retrieval.

3. Air mass trajectories

The trajectories of the air masses arriving at the AERONET sites in the ADRIEX study area, based on ECMWF operational analyses, are shown in Figure 1. The different coloured lines show the origin of the aerosol at different pressure levels. At the lowest two levels, 900 and 865 hPa, the air mass has passed over continental Europe, i.e. aerosol is advected from France over the Swiss and Austrian Alps, Northern Italy, and then for a very short time over the coastal Adriatic Sea. The trajectory at 700 hPa had a roughly similar course over the Alps but originated further south over the Mediterranean. Lidar measurements at Nicelli airport (see Figure 2) confirm the different nature of the upper-level aerosol, with some depolarization, whereas the lower-level aerosol is likely continentally polluted (Barnaba *et al.*, 2007). In view of the low wind speeds in the area around the time of overpass (less than 3 m s^{-1}), local generation of sea spray was unlikely.

4. AATSR/SEVIRI/AERONET intercomparison

Figure 2 shows the Northern Adriatic as seen by AATSR at 0955 UTC on 4 September 2004. The Venetian estuary is visible north of the cloud bank which stretches across the central region of the image. The Po Valley is the area between the two mountain ranges, the Apennines and the Alps. The blank area along the eastern side of the image is outside the AATSR swath.

DOI: 10.1002/qj

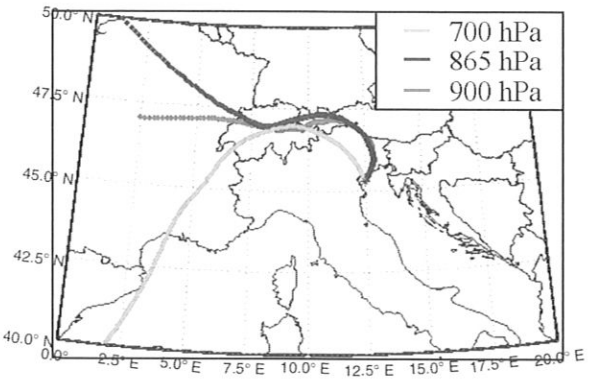

Figure 1. ECMWF model trajectories for the air above the Venice AERONET site on 4 September 2004. This figure is available in colour online at www.interscience.wiley.com/qj

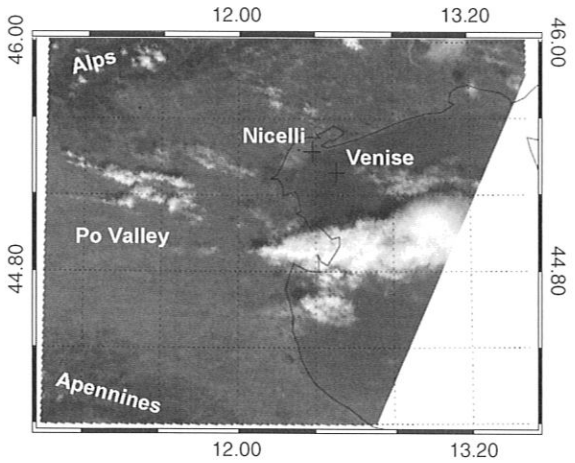

Figure 2. The view of the Northern Adriatic captured by AATSR (using the 0.87 μm channel) on 4 September 2004. Locations of the AERONET stations at the Venice Ocean Tower (Venise) and Nicelli Airport are indicated with crosses.

In the following sections we discuss the results given by each instrument/algorithm combination compared to the others and the AERONET optical depth values for the overpass time.

4.1. Direct comparisons with AERONET data

Tables 1 and 2 show the comparison of different instruments and algorithms with the Venice Ocean Tower and Nicelli AERONET sites respectively. Using a spatio-temporal averaging approach similar to that described by Ichoku *et al.* (2002), AERONET optical depths averaged over ±30 min of the satellite overpass have been compared to satellite optical depths averaged over ±20 km. There is no SEVIRI AERONET retrieval coincident with the AATSR overpass of the Nicelli Airport site as the coincident area was at the edge of a cloud bank and flagged cloudy. Aerosol class suggested by the ORAC results for both SEVIRI and AATSR was predominantly maritime, despite the continental origins suggested by the trajectories given in Figure 1.

All satellite retrievals retrieved a higher AOD than the AERONET AOD. For the Venice Ocean Tower AERONET site, the SEVIRI measurements produced the best overall match. This may be because the SEVIRI aerosol retrieval is less susceptible to sun-glint contamination in this part of the globe and may also have a more rigorous cloud flagging scheme. The optimal estimation results from both AATSR and SEVIRI perform better at the Venice Ocean Tower site than the dual-view algorithm, whereas at Nicelli Airport the dual-view algorithm shows better agreement with the AERONET value. However, when temporally/spatially averaged in this way, the results of all algorithms are within one standard deviation of each other.

4.2. AATSR ORAC retrieval results

The ORAC retrieval of AOD at 0.55 and 0.87 μm for this scene is displayed in Figure 3. Pixels flagged as cloud have been removed from the data and filtering based on the quality of fit given by the retrieval algorithm has been applied. There are some important features in this plot that warrant further explanation. Firstly, the retrieved optical depths over land are, on average, much higher than over the sea and are also higher than

Table I. Comparison of satellite AOD with Venice Ocean Tower AERONET AOD.

Algorithm	0.55 μm		0.67 μm		0.87 μm	
	AERONET	Satellite	AERONET	Satellite	AERONET	Satellite
ORAC/SEVIRI	0.15 ± 0.01	0.18 ± 0.07			0.058 ± 0.007	0.09 ± 0.04
ORAC/AATSR	0.15 ± 0.01	0.23 ± 0.04			0.058 ± 0.007	0.08 ± 0.03
TNO/AATSR	0.15 ± 0.01	0.24 ± 0.07	0.11 ± 0.01	0.18 ± 0.06		

Table II. Comparison of satellite AOD with Nicelli AERONET AOD.

Algorithm	0.55 μm		0.67 μm		0.87 μm	
	AERONET	Satellite	AERONET	Satellite	AERONET	Satellite
ORAC/AATSR	0.17 ± 0.01	0.39 ± 0.21			0.075 ± 0.003	0.25 ± 0.18
TNO/AATSR	0.17 ± 0.01	0.25 ± 0.09	0.12 ± 0.01	0.19 ± 0.09		

DOI: 10.1002/qj

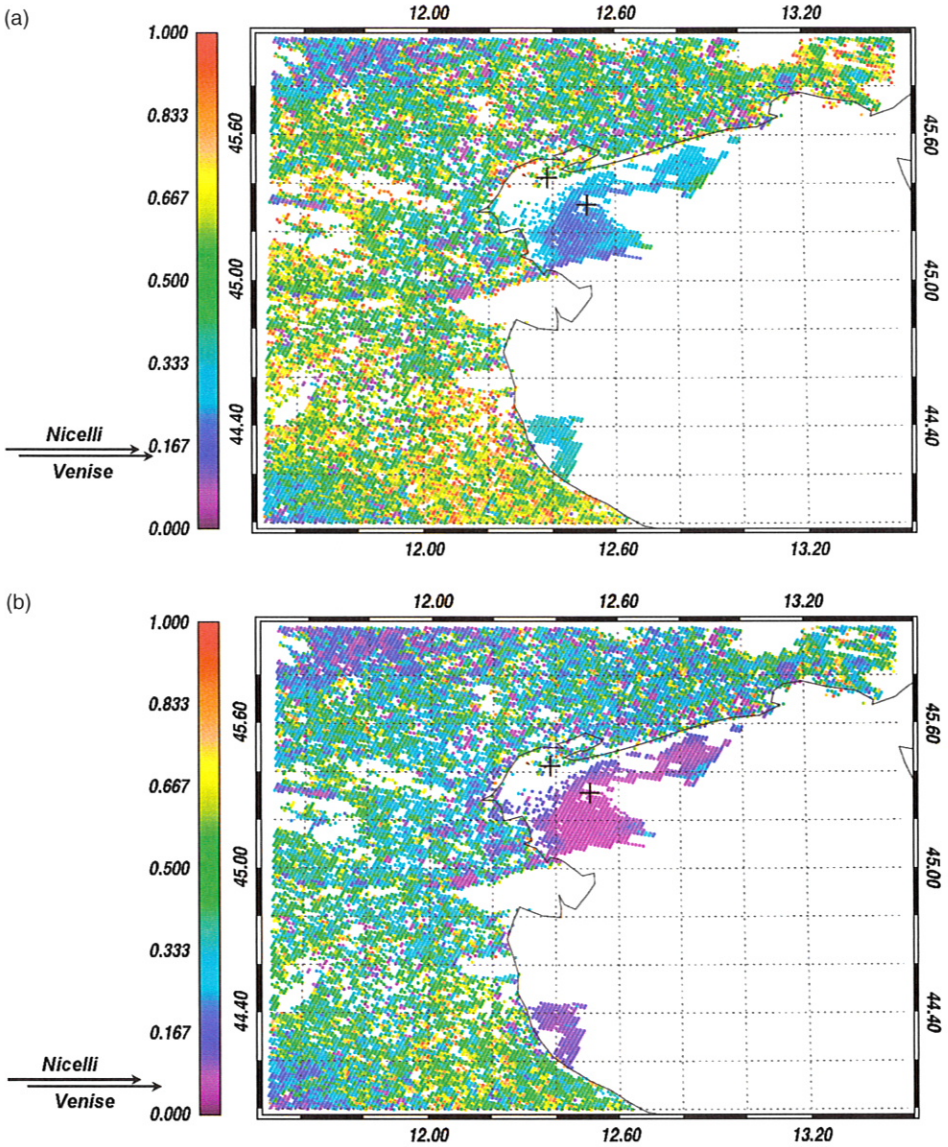

Figure 3. Aerosol optical depth maps at (a) 0.55 μm and (b) 0.87 μm, as calculated by the ORAC/AATSR combination. Each point corresponds to a 1×1 km pixel. The optical depths observed at the two AERONET stations are also indicated.

the corresponding values retrieved by the other satellite analyses presented here, as well as the AERONET measurements (see Table 2). There is also a larger variability in the optical depth over the land than over the ocean. Both of these demonstrate the limitations of the single-view approach used by the ORAC retrieval algorithm. Variations in the surface reflectance on a scale too small (both in space and time) to be captured by the MODIS BRDF product, as well as the limitations of the MODIS BRDF model itself, lead to significant errors in the aerosol properties retrieved by ORAC. This problem is compounded over brighter surfaces (such as urban areas and cultivated land) as the aerosol signal will constitute a small portion of the total TOA radiance detected and any inaccuracy in the description of the surface will be greatly magnified in derived aerosol properties. The absence of this problem is the main advantage of the TNO algorithm and it is hoped that inclusion of a dual-view capability in the ORAC algorithm will result in considerable improvements in its performance over the land (work which is currently under way).

It should also be noted that a large part of the eastern portion of the swath has been masked due to sun-glint contamination. ORAC uses a threshold on the Cox and Munk based ocean surface reflectance to mask areas of sun-glint (and, as the Cox and Munk reflectance is used in the retrieval, small changes in wind speed should be accounted for). However, the reliability of this method is limited by the accuracy of the ECMWF wind fields used to calculate the sea's roughness and there is some evidence of residual sun-glint affecting the eastern edge of the retrievals. Additionally, the AATSR/ORAC results are consistently slightly higher over the ocean than the value measured at the Venice Ocean Tower AERONET site, which is suggestive of a small positive bias over the ocean in this scene. The most likely explanation for this difference is that the surface reflectance is

DOI: 10.1002/qj

being underestimated in the ORAC retrieval. The ORAC scheme, as used here, is optimized for global processing of large volumes of AATSR data. The parametrization used to describe the ocean surface reflectance assumes deep ocean water. As we are viewing coastal water in this case, we can expect the water to be carrying a much higher sediment load than deep ocean waters, which will increase the surface reflectance. The retrieval accounts for the resulting increased radiance by increasing the aerosol loading. In the future the coincident MERIS ocean colour product could be used to adjust the ocean reflectance to improve AOD retrievals around the coast.

4.3. SEVIRI ORAC retrieval results

The optical depths obtained from an ORAC retrieval of SEVIRI AOD, equivalent to the ORAC/AATSR results displayed in Figure 3, are shown in Figure 4. The results have had cloud removed and have been filtered based on the quality control given by the retrieval algorithm. While the individual pixels are a lot larger for the SEVIRI instrument, the area covered is much larger and Europe is not affected by sun-glint contamination. The sparsity of data points is due to the cloud masking, i.e. if a pixel is suspected of cloud contamination it is removed. Consequently more pixels are removed due to a higher probability of the pixel viewing cloud. For instance, at the time of this aerosol comparison, no coincidence was found with the Nicelli AERONET site because of nearby cloud cover, while the AATSR instrument did have a coincidence.

SEVIRI does not have a 0.55 μm channel, hence the 0.87 μm optical depth is the more accurate (since the presence of the 0.81 μm channel better constrains the retrieval at this wavelength). It is clear that ORAC/SEVIRI is performing better than the ORAC/AATSR over land. Although there is again considerably more variability over land than over sea, this is much less pronounced in the SEVIRI results, and the discontinuity in the optical depth when moving from land to ocean,

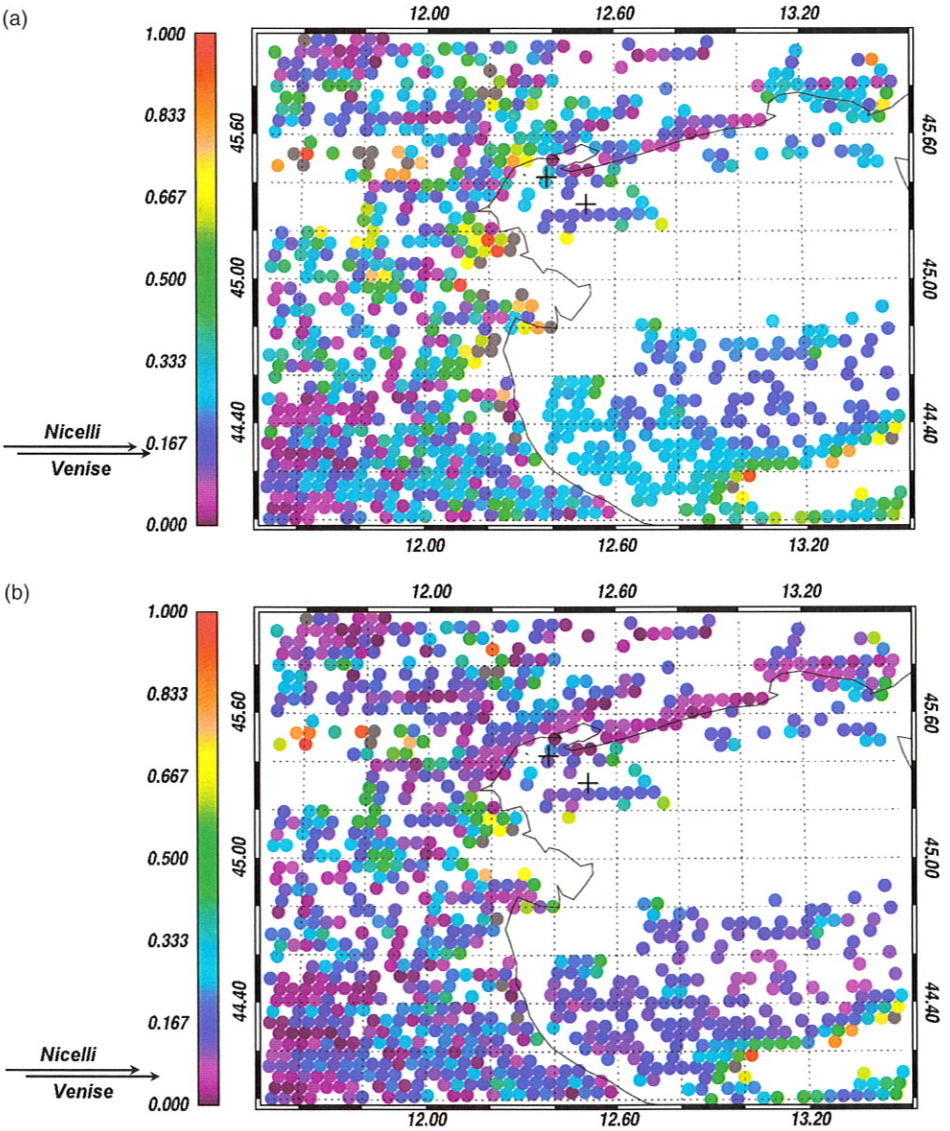

Figure 4. SEVIRI aerosol optical depth maps at (a) 0.55 μm and (b) 0.87 μm, as calculated using ORAC.

DOI: 10.1002/qj

apparent in the AATSR results, is not evident here. The better performance is most likely due to both the larger pixel size effectively smoothing out the anisotropic nature of the surface reflectance and the larger atmospheric path length, resulting in a stronger atmospheric signal, through which SEVIRI views the scene. (The viewing angle of SEVIRI at this latitude is approximately 45°.) Additionally, as SEVIRI does not have a 0.55 μm channel, the difference in the results could indicate a problem with the ORAC use of the MODIS BRDF product in this channel, possibly associated with its sensitivity to chlorophyll absorption. Indeed, tests have shown that if the AATSR retrieval is repeated with this channel excluded (i.e. the configuration of the SEVIRI retrieval is emulated), there is a decrease in the optical depth retrieved over many land pixels. However, due to the reduction of information in the measurement, there is a corresponding increase in the proportion of retrievals that fail to converge to a physically reasonable state.

There is some suggestion that SEVIRI is slightly overestimating the AOD; there is some evidence from Figure 4 that cloud contamination is an issue even though the ORAC algorithm has removed additional cloud to the operational SEVIRI cloud masking. The SEVIRI AOD is significantly larger at the edge of cloud banks and in some cases greater than 1.0. A new cloud flagging scheme will soon become operational at EUMETSAT, which should reduce some of the effects due to cloud contamination. Other improvements to be implemented in the SEVIRI ORAC algorithm include adopting the SEVIRI surface albedo product currently in development at EUMETSAT. In addition, since ocean colour measurements change on long time-scales compared to aerosol retrievals, it will be possible to remove the effects of changes in ocean colour with polar-orbiting ocean colour sensors, such as MERIS.

4.4. AATSR dual-view retrieval results

The corresponding TNO retrieval of AOD at 0.55 μm is displayed in Figure 5. The figure shows good agreement with the Nicelli AERONET data, with AATSR showing a slight bias towards higher optical depth. Agreement with the Venice Ocean Tower AERONET data is also good, although the bias is slightly larger than seen in the ORAC/AATSR retrievals. There is some variation of the optical depth over land, with high values occurring in the vicinity of clouds. Although some of this will be due to inaccurate cloud flagging, it is probable that some is also due to increasing humidity toward the clouds, resulting in aerosol growth and hence higher extinction. The areas of elevated optical depth are mostly confined to the Po Valley and the values vary smoothly over the Adriatic Sea coastline, i.e. there is little evidence of a sudden change in AOD values or patterns across the land–sea transition. However the TNO algorithm does show some unrealistic features along the eastern edge of the swath. Over the sea, these can be explained by sun-glint contamination since, in contrast to the ORAC algorithm, the TNO does not filter out sun-glint and it is not accounted for in the retrieval. However, artifacts are also visible over land pixels in the lower right-hand corner of the image that are clearly not due to sun-glint. A source of these artifacts has not been found and they seem to be a pecular feature of this specific scene, as similar artifacts have not been found in other scenes processed with the TNO algorithm.

Figure 6 shows the difference between the ORAC and TNO AATSR retrievals. The general overestimation and the unrealistic degree of scatter in the optical depth field given by the ORAC/AATSR combination is very apparent. However, over the ocean the two algorithms are more consistent, apart from the sun-glint-affected area along the eastern edge of the scan.

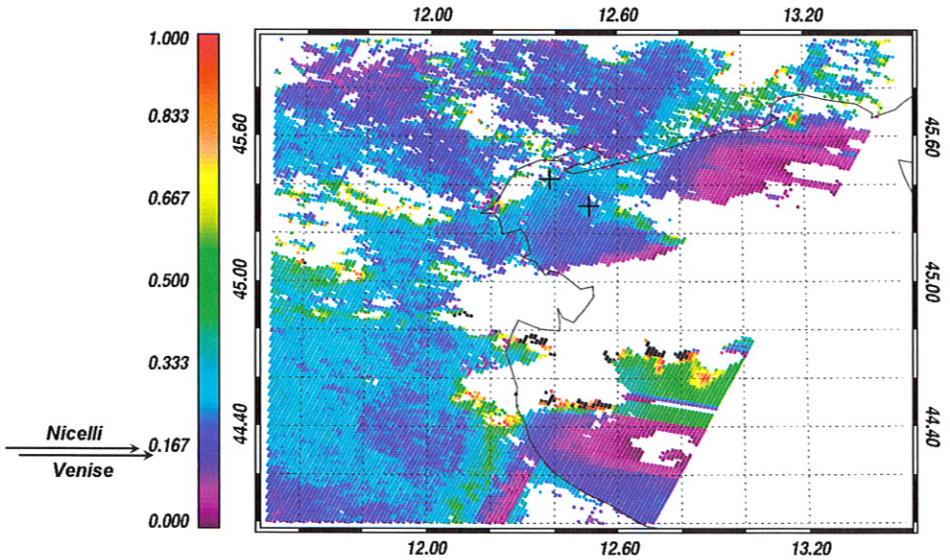

Figure 5. Aerosol optical depth map at 0.55 μm as calculated by the TNO/AATSR combination. Each point corresponds to a 1×1 km pixel.

DOI: 10.1002/qj

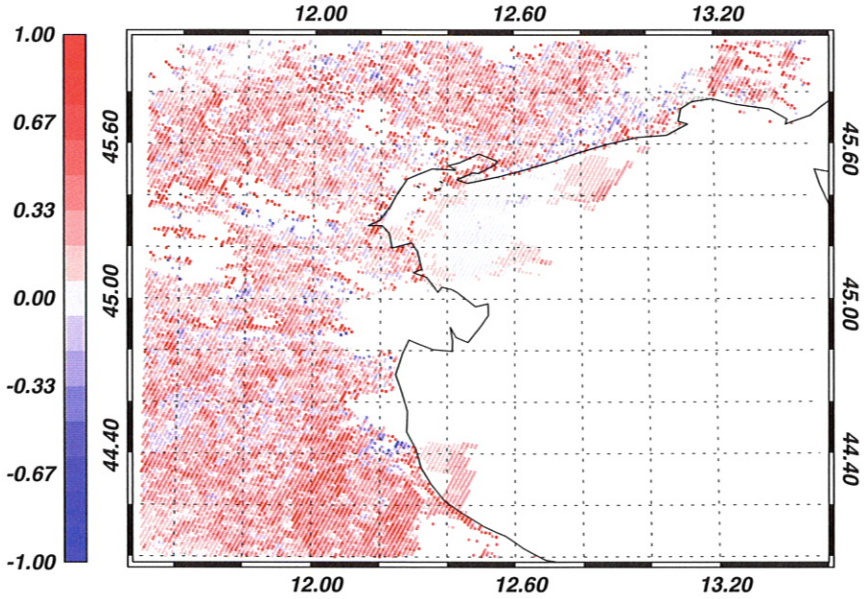

Figure 6. The difference between the results of the two AATSR algorithms (ORAC – TNO). Each point corresponds to a 1×1 km pixel.

5. Conclusions

Retrievals of aerosol optical depth for 4 September 2004 have been calculated using two instruments, the AATSR on board the Envisat polar-orbiting satellite and the SEVIRI instrument on board Meteosat-8, and using two techniques: a dual-view technique for AATSR and a single-view optimal estimation technique for AATSR and SEVIRI. The results in each case have been compared to each other and to two AERONET sites, Venice Ocean Tower and Nicelli Airport, which were operated during the ADRIEX aerosol measurement campaign.

The results for the TNO/AATSR and ORAC/SEVIRI cases were very encouraging with no obvious land/sea delineation. The ORAC/AATSR combination performed well over the ocean, but showed elevated optical depths in the Po Valley. Over the ocean site the satellite instruments measured within 0.1 AOD of the AERONET value in all cases. Over the land site (Nicelli) the single view ORAC/AATSR algorithm performed considerably worse than the dual-view TNO/AATSR method. This is to be expected, as the dual-view algorithm is less sensitive to assumptions on the surface reflectance. It is interesting to note that the single-view ORAC/SEVIRI algorithm performed much better than the ORAC/AATSR. As SEVIRI does not provide a 0.55 µm channel, this could point to a problem with the implementation of the MODIS BRDF product in defining the surface reflectance at this wavelength. ORAC/AATSR trials with the 0.55 µm channel disabled have shown that lower optical depths are indeed retrieved over the land. However, despite the reduction of the bias in the retrieved optical depths, the algorithm does not perform as well, with a greater number of failed retrievals. This high bias in ORAC optical depths over land is a clear indication that improvements are required in the ORAC forward model. Two improvements that will be implemented into the algorithm are the inclusion of a full bidirectional treatment of the surface reflectance and the ability to make use of the (A)ATSR dual-view measurement.

Compared with AERONET measurements, the dual-view TNO/AATSR retrieval showed a slight positive bias over both land and sea. Over sea the optimal estimation ORAC/AATSR retrieval performs slightly better, also with a slight positive bias, which can be partly attributed to the reflectance of these coastal waters being higher than that of the deep ocean water used in the ocean reflectance model. The SEVIRI optimal estimation retrieval showed a positive bias over sea but was more variable over land with an optical depth range of typically $\pm$ 0.1 about the mean. High optical depths were retrieved, as with other retrievals, around cloud edges. Over the ocean, the ORAC/AATSR algorithm provided a much closer match to the AERONET measurements in the 0.87 µm band than in the 0.55 µm one, with the relative differences being 35% at 0.55 µm and 28% at 0.87 µm.

Areas of improvement for all instruments and algorithm types have been identified. Comparison of the ORAC and TNO AATSR results strikingly show the power of the dual-view measurement system of the ATSR instruments. Comparing the single-view ORAC retrieval from AATSR with the dual-view TNO results graphically shows that, over the land, the *a priori* surface reflectance is the limiting factor in determining the accuracy of the single-view retrieval. This observation is further supported by the fact that the ORAC/AATSR combination seems to slightly outperform the ORAC/TNO retrieval over the ocean. The development of a ORAC algorithm that makes use of the AATSR dual view is under way and should greatly improve the retrieval's accuracy over land.

The assumptions made in utilizing the dual view in the TNO algorithm seem, on the basis of the results presented here, to be working well. The results do show the need

DOI: 10.1002/qj

for sun-glint flagging over the ocean, and also show signs of cloud contamination. However the unrealistic features seen over the land are a cause for concern and may point to a slight numerical instability in the algorithm, but it is important to note that this scene is the only one in which the TNO algorithm has produced such artifacts. It is hoped that further improvements to the analysis algorithms will allow this dataset, which now provides more than ten years of continuous measurement, to reach its full potential as a unique and reliable global aerosol dataset, both historical and ongoing.

Acknowledgements

We would like to thank Brent Holben and the AERONET principal investigators who allowed the use of the sun-photometer data that made the validation analysis possible. In particular we thank Giuseppe Zibordi who is the principal investigator of the Venice site. Robin Schoemaker is acknowledged for making the TNO dual-view code available. The work by RAL and Oxford in this paper is supported by the ESA Data User Element programme Globaerosol and the NERC UTGARD project. AATSR data were supplied by ESA under Category 1 proposal 2758 and the SEVIRI data were provided by EUMETSAT. The work by TNO presented in this paper is supported by the Netherlands User Support Programme GO-2, managed by SRON, project EO-065 (Validation of SCIAMACHY and OMI NO2 and aerosol data using Dutch ground-based measurements).

References

Aminou D, Jacquet B, Pasternak F. 1997. 'Characteristics of the Meteosat Second Generation Radiometer/Imager SEVIRI'. *Proceedings of SPIE*, Europto series **3221**: 19–31.

Barnaba F, Gobbi G-P, de Leeuw G. 2007. Aerosol stratification, optical properties and radiative forcing in Venice (Italy) during ADRIEX. *Q. J. R. Meteorol. Soc.* **133**(S1): 47–60.

Berk A, Bernstein LS, Anderson GP, Acharya PK, Robertson DC, Chetwynd JH, Adler-Golden SM. 1998. MODTRAN cloud and multiple scattering upgrades with application to AVIRIS. *Remote Sens. Environ.* **65**: 367–375.

Birks A, Llewellyn-Jones D, Buckley M, Fletcher M. 2004. *ESA AATSR Product Handbook,* Issue 1.2. ESA ESRIN: Rome.

Brindley HE, Ignatov A. 2006. Retrieval of mineral aerosol optical depth and size information from Meteosat Second Generation SEVIRI solar reflectance bands. *Remote Sensing Environ.* **102**: 233–363.

Cox C, Munk W. 1954. Measurements of the roughness of the sea surface from photographs of the sun's glitter. *J. Opt. Soc. Am.* **44**: 838–850.

De Haan JF, Bosma PB, Hovenier JW. 1987. The adding method for multiple scattering calculations of polarized light. *Astron. Astrophys.* **183**: 371–391.

Durkee PA, Jensen DR, Hindman EE, VonderHaar TH. 1986. The relationship between marine aerosols and satellite detected radiance. *J. Geophys. Res.* **91**: 4063–4072.

Flowerdew RJ, Haigh JD. 1995. An approximation to improve accuracy in the derivation of surface reflectances from multi-look satellite radiometers. *Geophys. Res. Lett.* **23**: 1693–1696.

Gordon HR, Wang M. 1994. Retrieval of water-leaving radiance and aerosol optical thickness over the oceans with SeaWiFS: A preliminary algorithm. *Appl. Opt.* **33**: 443–452.

Hess M, Koepke P, Schult I. 1998. Optical properties of aerosols and clouds: The software package OPAC. *Bull. Am. Meteorol. Soc.* **79**: 832–844.

Highwood EJ, Haywood JM, Coe H, Cook J, Osborne SR, Williams P, Crosier J, Bower K, Formenti P, McQuaid J, Brooks B, Thomas G, Grainger R, Barnaba F, Gobbi GP, de Leeuw G, Hopkins J. 2007. Aerosol Direct Radiative Impact Experiment (ADRIEX) overview. *Q. J. R. Meteorol. Soc.* **133**(S1): 3–15.

Holben BN, Eck TF, Slutsker I, Tanré D, Buis JP, Setzer A, Vermote E, Reagan JA, Kaufman YJ, Nakajima T, Lavenu F, Jankowiak I, Smirnov A. 1998. AERONET – A federated instrument network and data archive for aerosol characterization. *Remote Sensing Environ.* **66**: 1–16.

Höller R, Nagl C, Haubold H, Bourg L, d'Andon OF, Garnesson P. 2005. 'Evaluation of MERIS aerosol products for national and regional air quality in Austria'. Proceedings of MERIS–AATSR Workshop 2005, ESRIN, Italy. Available at: http://envisat.esa.int/workshops/meris_aatsr2005//participants/662/paper_hoeller.pdf.

Ichoku C, Chu DA, Mattoo S, Kaufman YJ, Remer LA, Tanré D, Slutsker I, Holben BN. 2002. A spatio-temporal approach for global validation and analysis of MODIS aerosol products. *Geophys. Res. Lett.* **29**: 1616, DOI: 10.1029/2001GL013206.

IPCC. 2001. *Climate Change 2001: The Scientific Basis. Contribution of Working Group I to the Third Assessment Report of the Intergovernmental Panel on Climate Change*. Houghton JT, Ding Y, Griggs DJ, Noguer M, van der Linden PJ, Dai X, Maskell K, Johnson CA. (eds.) Cambridge University Press: Cambridge and New York.

Jin Y, Schaaf CB, Woodcock CE, Gao F, Li X, Strahler AH, Lucht W, Liang S. 2003. Consistency of MODIS surface BRDF/Albedo retrievals: 1. Algorithm performance. *J. Geophys. Res.* **108**(D5): 4158, DOI: 10.1029/2002JD002803.

Kokhanovsky AA, Breon F-M, Cacciari A, Carboni E, Diner D, Di Nicolantonio W, Grainger RG, Grey WMF, Höller R, Lee K-H, North PRJ, Sayer A, Thomas GE, von Hoyningen-Huene W. 2007. Aerosol remote sensing over land: A comparison of satellite retrievals using different algorithms and instruments. *Atmos. Res.* in press.

Lohmann U, Feichter J. 2005. Global indirect aerosol effects: a review. *Atmos. Chem. Phys.* **5**: 715–737.

Martonchik JV, Diner DJ, Crean KA, Bull MA. 2002. Regional aerosol retrieval results from MISR. *IEEE Trans. Geosci. Remote Sensing* **40**: 1520–1531.

Mie G. 1908. Contribution to the optical properties of turbid media, in particular of colloidal suspensions of metals. *Ann. Phys. (Leipzig)* **25**: 377–452.

Mishchenko MI, Geogdzhayev IV, Cairns B, Rossow WB, Lacis AA. 1999. Aerosol retrievals over the ocean by use of channels 1 and 2 AVHRR data: sensitivity analysis and preliminary results. *Appl. Opt.* **38**: 7325–7341.

North PRJ. 2002. Estimation of aerosol opacity and land surface bidirectional reflectance from ATSR-2 dual-angle imagery: Operational method and validation. *J. Geophys. Res.* **107**: DOI: 10.1029/2000JD000207.

Remer LA, Kaufman YJ, Tanré D, Mattoo S, Chu DA, Martins JV, Li R-R, Ichoku C, Levy RC, Kleidman RG, Eck TF, Vermote E, Holben BN. 2005. The MODIS aerosol algorithm, products, and validation. *J. Atmos. Sci.* **62**: 947–973.

Robles Gonzalez C. 2003. 'Retrieval of aerosol properties using ATSR-2 observations and their interpretation'. PhD thesis, University of Utrecht, The Netherlands.

Robles Gonzalez C, Veefkind JP, de Leeuw G. 2000. Mean aerosol optical depth over Europe in August 1997 derived from ATSR-2 data. *Geophys. Res. Lett.* **27**: 955–959.

Robles Gonzalez C, de Leeuw G, Decae R, Kusmierczyk-Michulec J, Stammes P. 2006. Aerosol properties over the INDOEX campaign area retrieved from ATSR-2. *J. Geophys. Res.* **111**: D15, DOI: 10.1029/2005JD006184.

Rodgers CD. 2000. *Inverse methods for atmospheric sounding: Theory and practice.* World Scientific: Singapore.

Stammes P. 2001. Spectral radiance modelling in the UV–visible range. Pp 385–388 in *IRS 2000: Current problems in Atmospheric Radiation.* Smith WL, Timofeyev YM. (eds.) A. Deepak Publ: Hampton, Va, USA.

Stamnes K, Tsay SC, Wiscombe W, Jayaweera K. 1988. A numerically stable algorithm for discrete-ordinate-method radiative transfer in multiple scattering and emitting layered media. *Appl. Opt.* **27**: 2502–2509.

Stowe LL, Ignatov AM, Singh RR. 1997. Development, validation, and potential enhancements to the second-generation operational

aerosol product at the National Environmental Satellite, Data and Information Service of the National Oceanic and Atmospheric Administration. *J. Geophys. Res.* **102**: D14, 16 923–16 934.

Thieuleux F, Moulin C, Bréon FM, Maignan F, Poitou J, Tanré D. 2005. Remote sensing of aerosols over the oceans using MSG/SEVIRI imagery. *Ann. Geophys.* **23**: 3561–3568.

Thomas GE, Dean SM, Carboni E, Grainger RG, Poulsen CA, Siddans R, Kerridge BJ. 2007. 'An optimal estimation aerosol retrieval scheme for (A)ATSR'. Atmospheric, Oceanic and Planetary Physics Technical Memorandum 2007.1, University of Oxford, UK. Available at: http://www.atm.ox.ac.uk/main/research/technical/2007.1.pdf.

Veefkind JP, de Leeuw G. 1998. A new algorithm to determine the spectral aerosol optical depth from satellite radiometer measurements. *J. Aerosol Sci.* **29**: 1237–1248.

Veefkind JP, de Leeuw G, Durkee PA. 1998. Retrieval of aerosol optical depth over land using two-angle view satellite radiometry during TARFOX. *Geophys. Res. Lett.* **25**: 3135–3138.

Volz FE. 1972. Infrared refractive index of atmospheric aerosol substances. *Appl. Opt.* **11**: 755–759.

Watts PD, Mutlow CT, Baran AJ, Zavody AM. 1998. 'Study on cloud properties derived from Meteosat Second Generation observations'. ITT 97/181, EUMETSAT: Darmstadt, Germany.

DOI: 10.1002/qj